Calculated Droplet Size Distributions and Opacities of Condensed Sulfuric Acid Aerosols

James M. Wilder and Michael J. Pilat
University of Washington
Seattle, Washington

The properties of condensed polydisperse sulfuric acid aerosols in industrial flue gas were calculated. The condensed aqueous acid volume concentration, composition, droplet size distributions and condensed plume opacity were calculated for typical flue gas compositions, condensation nucleus size distributions and flue gas dilution ratios. The assumed initial flue gas at 170°C contained 0.035 g/acm fly ash particles, 1–20% water vapor, and 1–50 ppmv sulfuric acid vapor. The assumed gas cooling mechanism was by adiabatic dilution with cool ambient air. Polydisperse droplet growth was calculated by assuming equal surface area increase for each particle. The calculations show that sulfuric acid condensation should have minimal effect on particles larger than 1 μm, but will form a high concentration of particles in the narrow size range of 0.05–0.5 μm diameter. Depending on the initial sulfuric acid and water vapor concentrations in the hot flue gas, the calculated maximum plume opacity following gas dilution ranged from 5% to 25%, compared to 4% for the dry condensation nucleus aerosol.

The objective of this study was to mathematically investigate the influence of primary condensed sulfuric acid on the composition, size distribution, and opacity of particles in industrial and power plant emissions. An understanding of the mass concentration, size distribution, and opacity of condensed aerosols is important for developing strategies for the characterization, monitoring, control, and regulation of condensible emissions.

Hot flue gas from many industrial sources consists of inert gas, reactive gases such as sulfur dioxide, primary fly ash particles, and condensible vapors (primarily sulfuric acid and water vapor). The sulfuric acid vapor concentration is governed by the sulfur content in the process materials, the oxygen pressure in the gas stream during combustion, and the concentrations of catalytic elements in the gas stream. The flue gas is normally transported through ductwork at temperatures well above the expected sulfuric acid dewpoint to avoid corrosive acid deposition on duct walls or process equipment. However, eventually the flue gas must be cooled to ambient conditions, either by emission to the atmosphere or inadvertently by air leakage into ductwork. Upon gas cooling, the condensible sulfuric acid and water vapors may become supersaturated and form aqueous sulfuric acid droplets.

Several air pollution regulatory cases have involved the violation of local plume opacity emission standards by electric utility, petroleum refining, and nonferrous smelting operations. In some instances, these industries have reported that their dry particulate emissions are well within the allowable limits and that the plume opacity violations are caused by relatively small amounts of acid condensation in the dispersing plume. In these cases it is necessary to understand the formation mechanisms, aqueous composition, size distribution, and optical properties of aerosols formed by condensation of primary sulfuric acid onto polydisperse fly ash particles.

In a previous paper by Pilat and Wilder,[1] the formation mechanisms of primary sulfuric acid droplets in cooled industrial emissions were considered. In this paper, the condensed droplet size distributions and condensed plume opacities are calculated.

Review of Literature

Primary Sulfate Aerosol Studies. Measurements of condensed sulfuric acid droplet size distributions were made by Gillespie and Johnstone.[2] They used a prototype cascade impactor to sample generated hygroscopic aerosols and emissions from a sulfuric acid plant. They found that most of the condensed particle mass was contained in particles smaller than 2 μm. Chang and Tarkington[3] used a cascade impactor to measure nucleated sulfuric acid droplet size distributions from their high capacity acid aerosol generator. They observed that the mass median diameter was 0.3–0.6 μm and that virtually all of the particle mass was collected on the backup filter of their impactor. The observed droplet size distributions were not lognormal. Nader and Conner[4] compared in-stack condensible vapor concentrations, in-stack opacity, and near-stack opacity at oil fired and coal fired boilers. Observed plume opacity exceeded in-stack opacity when the flue gas temperature was above 150°C. They concluded that the increased plume opacity was caused by sulfuric acid droplet formation as the hot flue gas was cooled to below the acid dewpoint. Homolya[5] studied the influence of primary sulfate emissions on ambient aerosol properties near an isolated oil fired power plant. Observed visual range correlated well with ambient aerosol sulfate content. Homolya concluded that sulfate aerosol formation near the plant was directly influenced by primary sulfate emissions. Parungo *et al.*[6] measured ambient particle size distributions at various distances downwind from a copper smelter. They noted a fourfold increase in submicron particle concentrations after their collected samples were exposed to ammonia gas. They concluded that particles smaller than 0.5 μm diameter were coated with liquid sulfuric

acid. Pilat *et al.*[7] used X-ray analysis of cascade impactor samples to measure the size classified composition of particles from in-stack oil boiler emissions. Measured submicron particle concentrations were higher in samples taken at temperatures below the sulfuric acid dewpoint (roughly 110°C). X-ray analyses showed relatively high sulfur concentrations in submicron particles. Visual inspection of the impactor stages revealed the presence of liquid droplets (presumably aqueous sulfuric acid) only in low temperature samples between 0.1–0.7 μm diameter. They concluded that sulfuric acid condensation formed particles between 0.1–1 μm diameter when the flue gas was cooled to below the sulfuric acid dewpoint temperature. Dellinger *et al.*[8] measured sulfuric acid concentrations in high SO_2 emissions from a cement kiln. They found that high concentrations of calcium in the particles resulted in a low liquid pH, which in turn allowed significant amounts of SO_2 to H_2SO_4 oxidation to occur during the condensation and particle growth process. They concluded that for emissions from cement kilns, sulfuric acid concentrations and near-stack plume opacity can be significantly higher than would be expected by consideration of primary sulfate alone. Wilder *et al.*[9] measured the effects of primary sulfuric acid droplets on the particle size distributions and near-stack plume opacity of emissions from a copper smelter. Sulfate concentrations were consistently highest in particles between 0.3 and 1 μm diameter. They concluded that primary sulfuric acid condensation significantly influenced the size distributions of the emitted particles, and the maximum opacity of the near-stack plume.

Sulfuric Acid Droplet Formation Mechanisms. The mechanisms for gas to particle conversion of supersaturated water and sulfuric acid molecules to form aqueous acid droplets were modeled in previous studies.[1,10,11] There are three major mechanisms for droplet formation and growth: condensation of supersaturated molecules onto existing nuclei; homogeneous nucleation of sulfuric acid and water molecules to form small, pure liquid droplets; and coagulation of newly formed droplets. At gas temperatures and vapor concentrations typically found in industrial emissions, it appears that heterogeneous condensation onto existing nuclei should be the dominant droplet formation mechanism. For emission streams with acid vapor concentrations below 100 ppmv, the acid vapor depletion rate by condensation should be many orders of magnitude higher than the supersaturated vapor depletion rate by homogeneous nucleation. Nucleation should become the dominant vapor depletion mechanism only when the sulfuric acid vapor concentration exceeds roughly 100 ppmv.

Condensing Droplet Growth. Using theories developed by Langmuir,[12] many researchers have demonstrated the following relationship for polydisperse condensing droplet growth:

$$d_j^2 = a_j^2 + Y(t) \tag{1}$$

where d_j is the final droplet diameter following vapor condensation onto nuclei of initial diameter a_j. $Y(t)$ is a time dependent growth function that depends on the gas temperature and vapor concentrations, but which is independent of particle size. This relationship was demonstrated by Wilson and LaMer,[13] Sinclair and LaMer,[14] LaMer and Dinegar,[15] and LaMer *et al.*[16] during development of generators for monodisperse hydrosols and aerosols. They generated highly monodisperse droplets by condensing volatile vapors onto small nuclei and found that the polydispersity of the initial nuclei had little effect on the monodispersity of the final aerosols.

Condensation Nuclei Size Distributions. Lacey *et al.*[17] used an electric aerosol mobility analyzer to measure oil fired boiler emission particle distributions between 0.02 and 50 μm diameter. The measured particle concentrations were 48–140 mg/acm. They found relatively few particles smaller than 0.03 μm diameter. McCain[18] used an electric aerosol mobility analyzer and optical particle counters to measure coal fired boiler emission particle distributions between 0.01 and 1 μm diameter. The total particle number concentration was roughly 5 $\times 10^{13}$/acm. Number concentrations of particles smaller than 0.05 μm were very low, presumably because of particle coagulation upstream of the sampling point.

Calculation Procedures

Assumed Initial Flue Gas Properties. The initial hot flue gas was assumed to be similar to oil fired boiler emissions. The assumed initial temperature was 170°C, which is above the expected sulfuric acid dewpoint. The assumed initial water vapor and sulfuric acid vapor concentrations were 1–20% and 1–50 ppmv, respectively. The initial flue gas was assumed to contain polydisperse fly ash with size distributions similar to those measured by Lacey *et al.*[17] For this model, the fly ash was assumed to be spherical and inert. The total initial particle mass concentration was 0.035 g/acm at 170°C. To investigate the influence of submicron nucleus size distribution on final droplet properties, two initial particle size distributions were used. Each used the same total mass concentration, but the total particle number concentrations were 2×10^{13} and 1.1×10^{14} particles/acm, respectively, for the two distributions.

Flue Gas Cooling. For this model, it was assumed that the 170°C flue gas was cooled by adiabatic dilution with 15°C ambient air. Such dilution would certainly occur following discharge from a stack, but inadvertent dilution could also occur by air leakage into ducts and process equipment. The extent of gas dilution was specified by the ratio:

$$\text{Dilution ratio} = \frac{\text{Volume of dilution air @ } T_d}{\text{Initial flue gas volume @ } T_i} \tag{2}$$

where T_i and T_d are the absolute temperatures of the initial flue gas and the ambient dilution air.

The final gas temperature T_f following dilution and sulfuric acid condensation was calculated using an energy balance between the initial and diluted/cooled gas states:

$$\begin{aligned}\text{Flue gas enthalpy} + \text{Dilution air enthalpy} &= \text{Inert gas enthalpy} \\ &+ \text{Condensed liquid enthalpy} \\ &+ \text{Latent heats of vaporization}\end{aligned} \tag{3}$$

$$T_f = \frac{m_i C_{pi} T_i + m_d C_{pd} T_d - m_w \Delta H_w - m_a \Delta H_a}{m_g C_{pg} + m_w C_{pw}} \tag{4}$$

where m_i, m_d, and m_g are the masses of initial flue gas, dilution air, and uncondensed inert gas (g/acm), m_w and m_a are the mass of condensed liquid water and H_2SO_4 (g/acm); C_{pi}, C_{pd}, C_{pg} and C_{pw} are the heat capacities (cal/g°K) of the flue gas, dilution air, inert gas and liquid water; and ΔH_w and ΔH_a are the heats of vaporization for pure H_2O and H_2SO_4.

Condensed Sulfuric Acid Properties. The aqueous composition and volume concentration of the sulfuric acid condensed following flue gas cooling were calculated using the equilibrium computational technique developed in earlier studies.[1,10,11] For assumed flue gas water vapor and acid vapor concentrations, the aqueous acid composition (weight % H_2SO_4) and condensed liquid volume (μ^3/acm) were calculated using iterative solutions for H_2O and H_2SO_4 mass balances. Equilibrium vapor pressure data were from Gmitro and Vermeulen.[19]

Droplet Growth Calculations. The final acid droplet diameters d_j, following condensation onto initial nuclei with diameter a_j, were calculated by assuming that during the condensational growth process the surface area of each particle increases by an identical amount, regardless of the initial

polydisperse nucleus diameter. This principle is expressed by the equilibrium relationship:

$$d_j^2 = a_j^2 + Y \quad (5)$$

where the equilibrium growth factor Y is independent of the initial nucleus diameter a_j. After the growth factor was calculated by an iterative process, the final condensed droplet diameters d for each size class j were computed by using Eq. 5. The assumed initial nucleus density was 2.5 g/cm^3 and the aqueous acid density was 1–1.8 g/cm^3, depending on the gas temperature.

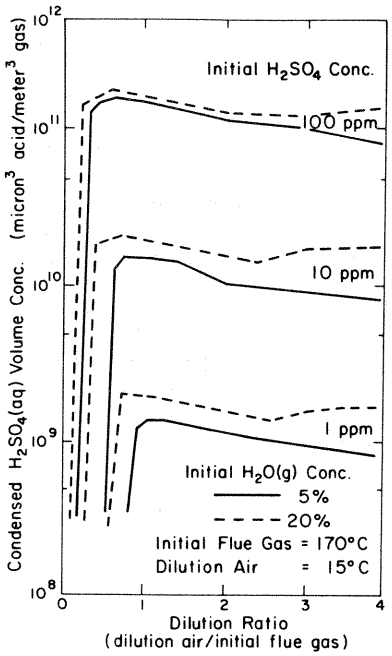

Figure 1. Calculated condensed H_2SO_4(aq) volume as a function of flue gas dilution.

Kelvin Effect Considerations. The influence of droplet curvature on equilibrium vapor concentrations above the condensed aqueous solutions should have little effect on calculated droplet size distributions. For the gas temperatures specified for this model, the Kelvin effect would cause a vapor pressure increase of only 1% for 0.1 μm droplets, as reported in an earlier study.[1] This slight vapor pressure increase would negligibly affect the equilibrium droplet size calculations. Furthermore, any preferential evaporation of smaller droplets (which has been predicted to happen in the stratosphere[20]) should not be significant during the short residence time of the condensed droplets in the emissions.

Condensed Particle Coagulation. Changes in condensed droplet size distributions due to particle coagulation were estimated using the modified Smulochowski calculations developed by Hogan.[21] Polydisperse coagulation rates were estimated by assuming that the condensed droplets acted as spheres, with a density of 1.8 g/cm^3.

Condensed Plume Opacity. The opacity of the polydisperse condensed aerosol was estimated using Mie light scattering theory, assuming that the condensed droplets were pure light scatterers. Opacity was calculated using the Beer-Lambert law:

$$\% \text{ Opacity} = 100[1 - \exp(-B_{ext}L_p)] \quad (6)$$

where B_{ext} is the light extinction coefficient (m^{-1}) and L_p is the light pathlength (m). For a polydisperse aerosol, B_{ext} is a function of the particle size distribution, incident light wavelength λ, and the particle refractive index xm:

$$B_{ext} = \sum \frac{\Pi}{4} d_j^2 N_j Q_{ext}(d_j,\lambda,xm) \quad (7)$$

where $Q_{ext}(d_j,\lambda,xm)$ is the effective light extinction efficiency factor and N_j is the nucleus concentration. For this model, the efficiency factor Q_{ext} was estimated using the calculation procedure developed by Ensor and Pilat.[22] A single light wavelength (λ = 0.55 μm) was used and the particle refractive index was assumed to be 1.43.

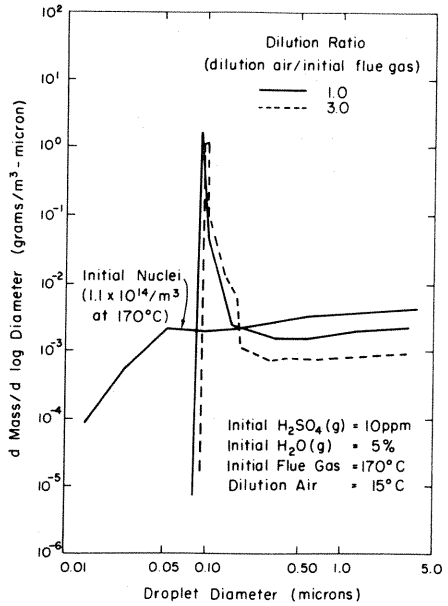

Figure 3. Calculated droplet size distributions for two flue gas dilution ratios.

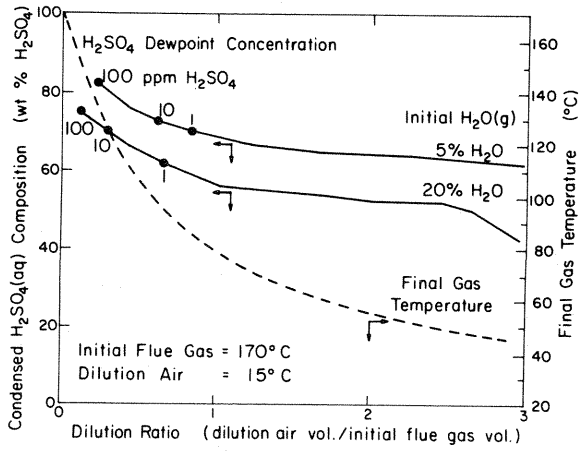

Figure 2. Calculated condensed H_2SO_4(aq) composition as function of gas dilution ratio.

Calculated Results

Condensed Sulfuric Acid Properties. The volume of aqueous sulfuric acid condensed after the 170°C flue gas was diluted and cooled with 15°C ambient air is shown in Figure 1. The calculated acid volume concentrations are shown for two initial H_2O(g) concentrations (5 and 20%) and three initial H_2SO_4(g) concentrations (1, 10, and 100 ppm) as a function of the flue gas dilution ratio. Figure 1 illustrates the following:

1) Acid condensation should not occur until the flue gas has been cooled to below the H_2SO_4-H_2O system dewpoint which corresponds to a dilution ratio in the 0.2–1 range.

2) After the acid dewpoint is reached and condensation begins, the condensed acid volume concentration should increase rapidly to some maximum value. Additional dilution of the flue gas beyond that point results in little additional acid condensation.
3) For a specified gas dilution ratio, the condensed acid volume concentration should be nearly proportional to the initial H_2SO_4(g) concentration in the flue gas.

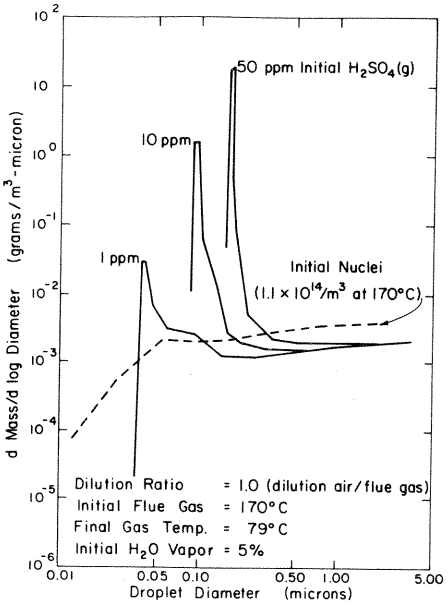

Figure 4. Calculated droplet size distributions for three initial H_2SO_4(g) concentrations.

The composition of the liquid sulfuric acid as a function of the flue gas dilution ratio is shown in Figure 2. Points for the sulfuric acid dewpoint concentrations of 1, 10, and 100 ppm are shown for two initial H_2O concentrations of 5 and 10%. Figure 2 shows the following:

1) The H_2SO_4-H_2O system dewpoint depends upon the initial H_2O(g) and H_2SO_4(g) concentrations. The acid dewpoint temperature increases with higher H_2SO_4(g) concentrations and increases with higher water vapor concentrations.
2) Below the acid dewpoint temperature the condensed acid composition is nearly independent of the initial H_2SO_4(g) concentration and is dependent upon the initial H_2O(g) concentration and the dilution ratio (or gas temperature).
3) The condensed acid concentration is highest at temperatures just below the dewpoint and decreases with further gas dilution.

Calculated Droplet Size Distributions. Calculated final droplet size distributions for the aerosols formed by acid condensation onto fly ash particles are shown in Figure 3. The original fly ash distribution and condensed droplet distributions are shown for two different gas dilution ratios. Inspection of this figure shows the following:

1) Acid condensation should have little effect on fly ash particles larger than roughly 0.5 μm diameter. Relative condensational growth of large particles is minimal so gas dilution simply reduces large particle concentrations without changing the shape of the particle distribution curve above roughly 0.5 μm.
2) Acid condensation onto very small fly ash particles (smaller than roughly 0.05 μm) should form very nearly monodisperse acid droplets in the narrow 0.05–0.2 μm size range. The resultant overall size distribution between 0.05 and 5 μm diameter might be considered to consist of two parts: a nearly monodisperse droplet aerosol between 0.05 and 0.2 μm diameter superimposed onto a diluted but otherwise unchanged aerosol of fly ash particles larger than 0.5 μm.
3) Note that the nearly monodisperse droplets are on the fringe of the optically active particle size range, 0.1–1 μm diameter. It should be anticipated that condensed acid aerosols will be efficient light scatterers.

Calculated condensed droplet size distributions as a function of flue gas acid vapor concentration are shown in Figure 4. The assumed flue gas dilution ratio is 1 m^3/m^3, at which point the condensed acid volume is near the maximum value (see Figure 1). Inspection of Figure 4 shows the following:

1) Even for very high sulfuric acid vapor concentrations, acid condensation following gas cooling should have a minimal effect on fly ash particles larger than roughly 0.5 μm diameter.
2) The size and mass concentration of the nearly monodisperse condensed droplets smaller than 0.5 μm will be strongly influenced by the initial acid vapor concentration. The final diameter and mass concentration of the small droplets will both increase with higher initial sulfuric acid vapor concentration. This follows directly from the fact that the volume of condensed aqueous acid is proportional to the initial acid vapor concentration (see Figure 1). For a fixed number of condensation nuclei, the volume of liquid per nucleus and hence the size of the liquid droplets will thus increase with higher acid vapor concentration.

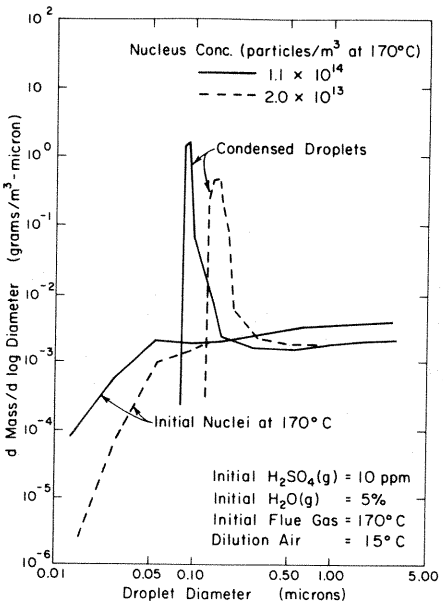

Figure 5. Calculated droplet size distributions for two initial nuclei size distributions.

Calculated condensed droplet size distributions for a dilution ratio of 1 and an initial H_2SO_4(g) concentration of 10 ppm after condensation onto two initial nuclei size distributions are shown in Figure 5. It appears that the condensed droplet size distribution is significantly influenced by the nuclei size distribution below 0.1 μm diameter. If the condensed acid is essentially evenly distributed onto all nuclei smaller than about 0.05 μm diameter, then the final diameter of the monodisperse droplets should be nearly inversely proportional to the cube root of the total nuclei number concentration (which is generally governed by the nuclei distribution below 0.05 μm diameter).

Coagulation of sulfuric acid droplets following condensational growth should not necessarily influence the droplet size distributions. The condensation process itself is rapid enough so that coagulation during initial particle growth should be minimal. After condensation, the nearly monodisperse acid droplets are large enough so that their coagulation rates are relatively low. Using the procedures developed by Hogan,[21] coagulation rates were estimated for the following conditions: 10 ppmv initial acid vapor, 5% water vapor, and a gas dilution ratio of 1. The droplet size distribution for this aerosol after condensation was shown in Figure 3. Immediately after condensation, the calculated droplet concentration peak was at a droplet size of 0.094 μm. After 10 seconds of droplet coagulation, the concentration peak shifted to roughly 0.15 μm. After 60 seconds, the concentration peak shifted to 0.22 μm. These coagulation rates are relatively slow compared to the plume dilution rates caused by atmospheric dispersion. Droplet coagulation should therefore only minimally influence the near-stack size distributions in emission plumes. However, it is possible that condensed droplet size distributions for in-duct gas streams could be changed by droplet coagulation.

Condensed Aerosol Opacity. The condensed aerosol opacities were estimated by applying Mie light scattering calculations to the known condensed droplet size distributions. The assumed condensed particle refractive index was 1.43 and the assumed light pathlength was 5 m. Calculated opacities for dilution of the initial 170°C flue gas with various amounts of ambient air are shown in Figure 6. The calculated opacities are shown as functions of the gas dilution ratio for three values of initial sulfuric acid vapor concentration (0, 10, and 20 ppmv) and two initial condensation nucleus size distributions. Inspection of Figure 6 shows the following:

1) The opacity of the assumed initial flue gas, prior to gas dilution and condensation, was roughly 7% for the specified 5 m light pathlength.
2) Initial gas dilution ratios below roughly 0.3 m^3 dilution air/m^3 flue gas did not cool the flue gas to below the acid dewpoint. After the dewpoint was reached, continued gas dilution should cause rapid acid condensation with a rapid rise in plume opacity. For high acid vapor concentrations and low nucleus number concentrations, the condensed plume opacity could increase to well above 20% opacity.
3) For the gas conditions specified for this model, additional gas dilution beyond a dilution ratio of roughly 1 did not cause additional acid condensation. Therefore, large amounts of gas dilution simply reduced condensed particle concentrations and lowered the condensed plume opacity.

As seen in Figure 6, the calculated condensed plume opacity was much higher when the specified initial nucleus number concentration was low. For this model, two different initial nucleus size distributions were investigated. Each had a total mass concentration of 0.052 g/acm, but the total number concentrations for the two distributions were 2×10^{13} and 1.1×10^{14} particles/m^3. For a specified initial $H_2SO_4(g)$ concentration of 10 ppmv, the calculated maximum opacities after condensation onto the high concentration vs. low concentration nuclei were 6.5% vs. 11%, respectively. Similar results were calculated for 20 ppm initial $H_2SO_4(g)$ concentration: the peak opacities for the high and low concentration nuclei were 11% vs. 26%, respectively.

Based on this number concentration vs. opacity relationship, it is conceivable that installation of particulate control devices on emissions with high acid vapor concentrations could actually cause an increase in near-stack plume opacity. If the control device were installed at a point where the flue gas temperature was above the dewpoint, then the device would reduce the mass and number concentration of potential condensation nuclei without reducing the condensible vapor

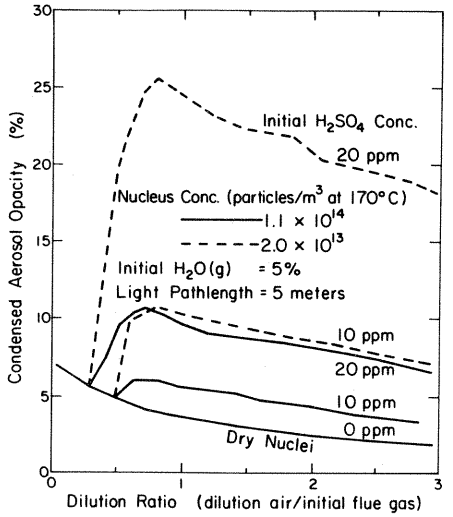

Figure 6. Condensed aerosol opacity as a function of gas dilution.

concentrations. As seen in Figure 6, such a reduction in nucleus concentrations could cause significant increases in the maximum opacity of the condensed emission plume.

Calculated condensed plume opacities as functions of initial acid vapor and water vapor concentrations are shown in Figure 7. In this figure the specified gas dilution ratio was 1, at which point the condensed plume opacity was near the maximum

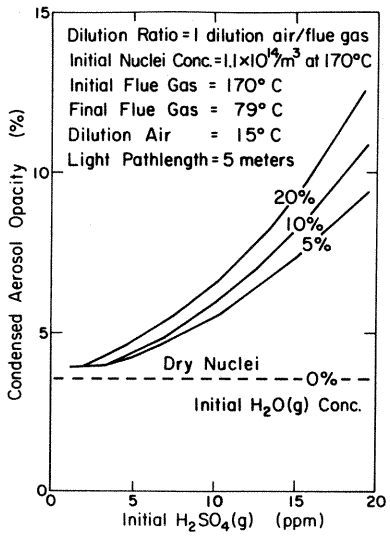

Figure 7. Effect of initial $H_2SO_4(g)$ on condensed aerosol opacity.

value (see Figure 6). Inspection of Figure 7 shows the following:

1) If no liquid condensation occurred, the calculated plume opacity was only 4% for the specified 5 m pathlength.
2) The calculated opacity is strongly influenced by the initial acid vapor concentration. For an initial acid vapor concentration of 20 ppm the calculated plume opacities were 9.5–12.5%, depending on the specified water vapor concentration.
3) The condensed plume opacity is also influenced by the initial water vapor in the hot flue gas, but the dependence on water vapor is not as strong as that for sulfuric acid vapor.

Conclusions

The calculated sulfuric acid dewpoint temperature depends on the initial concentrations of water vapor and acid vapor in the flue gas. The condensed aqueous acid composition depends mainly on the initial water vapor concentration. For the conditions studied, the calculated aqueous acid concentrations ranged from 40% to 80% H_2SO_4 by weight. The volume concentration of condensed liquid following gas cooling depends mainly on the initial acid vapor concentration in the flue gas.

Calculated droplet size distributions depend on the initial flue gas vapor concentrations, the initial nucleus number concentration, and the specified gas dilution ratio. Initial fly ash nuclei larger than roughly 1 μm should be unaffected by acid condensation. However, acid condensation onto initial particles smaller than 0.05 μm should create a high concentration of nearly monodisperse liquid droplets, in the narrow size range between 0.15 and 0.5 μm. The overall condensed droplet size distribution might be considered to consist of two components: essentially monodisperse liquid droplets between 0.15 and 0.5 μm diameter, superimposed onto diluted but otherwise unchanged particles larger than 1 μm.

The diameter and mass concentration of the 0.15–0.5 μm liquid droplets should both increase with higher acid vapor concentration in the initial flue gas. However, the diameter of the liquid droplets should decrease with higher condensation nucleus number concentrations in the flue gas.

The calculated condensed plume opacity depends on the flue gas condensible vapor concentrations, the condensation nucleus number concentration, and the extent of gas dilution/cooling. Maximum condensed plume opacity should increase significantly for higher acid vapor concentrations in the flue gas, and should increase slightly for higher water vapor concentration. The maximum plume opacity should depend very strongly on the number concentration of condensation nuclei in the flue gas.

Acknowledgments

This research was partially funded by the U.S. Environmental Protection Agency Air Pollution Training Grant No. T901355.

References

1. M. J. Pilat, J. M. Wilder, "Opacity of monodisperse sulfuric acid aerosols," *Atmos. Environ.* **17:** No. 9 (1983), to be published.
2. G. R. Gillespie, H. F. Johnstone, "Particle-size distributions in some hygroscopic aerosols," *Chem Eng. Prog.* **51:** 74 (1955).
3. D. P. Chang, B. K. Tarkington, "Experiences with a high output sulfuric acid aerosol generator," *Am. Ind. Hyg. Assoc. J.* **38:** 493 (1977).
4. J. S. Nader, W. D. Conner, "Impact of Sulfuric Acid Emissions on Plume Opacity," in *Workshop Proceedings on Primary Sulfate Emissions from Combustion Sources*, EPA-600/9-78-020b, U.S. Environmental Protection Agency, 1978, pp. 121–136.
5. J. B. Homolya, "Observations of aerosol composition and visibility near an isolated power plant," *Atmos. Environ.* **13:** 1099 (1979).
6. F. Parungo, R. Pueschel, E. Ackerman, H. Proulx, D. Wellman, *Characteristics and Meteorological Aspects of Pollutants from the Kennecott Copper Smelter*, NTIS No. PB 285995, National Technical Information Service, Washington, DC, 1978.
7. M. Pilat, J. Thielke, G. Raemhild, "Plume Opacity Related to Aerosol Composition in an Oil-Fired Boiler," Progress Report EPA Grant R803897, Department of Civil Engineering, University of Washington, Seattle, WA, 1978.
8. B. Dellinger, G. Grotecloss, C. Fortune, J. Cheney, J. Homolya, "Sulfur oxide oxidation and plume formation at cement kilns," *Environ. Sci. Technol.* **14:** 1244 (1980).
9. J. Wilder, T. Tucker, R. Welch, "Chemical Characterization of Visible Plumes from a Copper Smelter," presented at APCA Pacific Northwest International Section Annual Meeting, Vancouver, B.C., November 1982.
10. J. M. Wilder, "Theoretical Droplet Size Distributions and Opacities of Sulfuric Acid Aerosols," M.S. Civil Engineering Thesis, University of Washington, Seattle, WA, 1981.
11. J. Wilder, M. Pilat, "Size Distributions and Opacities of Condensed Sulfuric Acid Aerosols," presented at APCA Pacific Northwest International Section Annual Meeting, Yakima, WA, November 1980.
12. I. Langmuir, "The evaporation of small droplets," *Phys. Rev.* **12:** 363 (1918).
13. D. Sinclair, V. LaMer, "Light scattering as a measure of particle size of aerosols," *Chem. Rev.* **44:** 245 (1948).
14. I. Wilson, V. LaMer, "The retention of aerosol particles in the human respiratory tract," *J. Ind. Hyg. Toxicol.* **30:** 265 (1948).
15. V. LaMer, R. Dinegar, "Theory, production and mechanisms of formation of monodispersed hydrosols," *J. Am. Chem. Soc.* **72:** 4847 (1950).
16. V. LaMer, E. Inn, I. Wilson, "Methods of forming, measuring and detecting liquid aerosols in the size range 0.01–0.25 microns," *J. Colloid Sci.* **5:** 471 (1950).
17. G. E. Lacey, K. Cushing, W. Smith, *Compact, In-Stack 3 Size Cut Particle Classifier*, EPA 600/7-77-033, U.S. Environmental Protection Agency, 1977.
18. J. D. McCain, *CEA Variable Throat Venturi Scrubber Evaluation*, EPA/600/7-78-064, U.S. Environmental Protection Agency, 1978.
19. J. I. Gmitro, T. Vermeulen, "Vapor-liquid equilibria for aqueous sulfuric acid," *AIChE J.* **10:** 740 (1964).
20. G. K. Yue, "The formation and growth of sulfate aerosols in the stratosphere," *Atmos. Environ.* **15:** 549 (1981).
21. A. W. Hogan, "A simplified aerosol coagulation model," *JAPCA* **27:** 759 (1977).
22. D. S. Ensor, M. Pilat, "Calculation of smoke plume opacity from particulate air pollutant properties," *JAPCA* **221:** 496 (1971).

James M. Wilder and Michael J. Pilat are with the Department of Civil Engineering, University of Washington, Seattle, WA 98195. This paper was submitted for editorial review on May 12, 1982; the revised manuscript was received on June 27, 1983.